NASA CONTRACTOR REPORT

NASA CR-416

NASA CR-416

EXPERIMENTS ON THE IMPACT-LIGHT-FLASH AT HIGH VELOCITIES

by J. F. Friichtenicht

Prepared under Contract No. NASw-936 *by*
TRW SYSTEMS
Redondo Beach, Calif.
for

NATIONAL AERONAUTICS AND SPACE ADMINISTRATION - WASHINGTON, D. C. - MARCH 1966

NASA CR-416

EXPERIMENTS ON THE IMPACT-LIGHT-FLASH AT HIGH VELOCITIES

By J. F. Friichtenicht

Prepared under Contract No. NASw-936 by
TRW SYSTEMS
Redondo Beach, Calif.

for

NATIONAL AERONAUTICS AND SPACE ADMINISTRATION

For sale by the Clearinghouse for Federal Scientific and Technical Information
Springfield, Virginia 22151 – Price $0.45

EXPERIMENTS ON THE IMPACT-LIGHT-FLASH AT HIGH VELOCITIES

I. INTRODUCTION

One of the observable phenomena associated with hypervelocity impact is the so-called impact light flash produced by the conversion of some fraction of the projectile kinetic energy to radiant energy. The light flash provides a mechanism for the observation of high-speed impact phenomena. In addition, it has been used as a meteoroid counter in micrometeoroid detector systems,[1] and it is hoped that some property of the impact flash may be used in such systems to determine meteoroid mass and velocity. In this context Rosen and Scully[2] have suggested that photometric measurements of the impact flash at two different wavelengths may provide the desired information.

Traditionally, the depth of penetration and the size of craters formed have been the most significant engineering parameters of high-velocity impact, and by far the bulk of experimental and theoretical work has been concerned with these aspects of high-speed impact. The effects of melting and vaporization have only recently been considered in hypervelocity penetration theory.[3] Some properties of the vapor cloud can be observed directly by photographic techniques,[4] while others may be inferred from indirect measurements such as those of ionization processes.[5] The existence of ionization suggests that the vapor cloud may possess plasma-like characteristics, including self-luminosity due to the excitation of neutral gas atoms. Thus quantitative measurements of the properties of the impact light flash can provide information on vaporization effects.

In an early study[6] of the impact light flash conducted with large projectiles from a light gas gun, line spectra arising from excitation of residual gas atoms in the target chamber appeared to account for most of the observed radiation. The more

recent experiments of Rosen and Scully (Ref. 2) were conducted in a vacuum of less than 10^{-2} mm Hg using small projectiles approximately 50 microns in diameter. Since the residual gas interactions were negligible, the observed radiation was attributed to blackbody emission from heated particles or droplets ejected from the target. On the basis of this assumption, they were able to correlate the peak flash intensity with the amount of material ejected from the target.

This report describes experiments on the impact light flash conducted with very small (approximately 1 micron) particles over the velocity range from about 2.5 km/sec up to nearly 40 km/sec. The results of measurements using unfiltered photomultiplier tubes suggested that the emission spectrum was similar to that of a blackbody radiator. Apparent blackbody temperatures were measured by two-color photometric techniques similar to those used by Rosen and Scully, and similar results were obtained over the range of velocities common to both experiments. However, a significant departure from the rate of increase of temperature with velocity predicted by Rosen and Scully was observed. Although no attempt has been made to determine the source of radiant energy, it appears likely that two sources exist: One is blackbody emission from heated material, the other radiation from excited atoms in the vapor cloud.

II. EXPERIMENTAL PROCEDURES

A. Particle Acceleration and Analysis

In all of the work discussed here the TRW Systems electrostatic hypervelocity accelerator[7] was used. In this accelerator small particles are first charged electrically by a process described elsewhere[8] and then injected into the accelerating electric field of a 2-million-volt Van de Graaff Generator. Here they are accelerated to a final velocity given by $v = (2qV/m)^{1/2}$, where V is the accelerating voltage, m is the mass of the particle,

and q is its charge. As described in Ref. 8, the q/m of a particle is proportional to the reciprocal of the particle radius. As a consequence of this relationship, the electrostatic method of accelerating particles is most effective for very small particles. Under optimum conditions, iron particles of 1 micron diameter reach a final velocity of about 7 km/sec. (Smaller particles, or particles composed of lower density materials, achieve correspondingly higher velocities. As examples, carbon particles have been accelerated to velocities in excess of 20 km/sec, and submicron iron particles have been accelerated to nearly 40 km/sec.) Carbonyl iron spheres (98% Fe) with a mean diameter of about 1.5 microns were used for all of the experiments described below.

The charge and velocity of each particle are determined after it has been accelerated but before it strikes the target surface. This is accomplished by measuring the magnitude and duration of the voltage signal induced by a particle as it passes through a cylindrical drift tube of known capacitance and length. The charge is given by $q = CV_i$, where V_i is the amplitude of the induced voltage pulse and C is the capacitance of the drift tube to ground. The velocity is simply $v = \ell/t$, where t is the transit time through a cylinder of length ℓ. The mass of the particle is found from $m = 2qV/v^2$.

Usually the signal from the detector is amplified and displayed on an oscilloscope trace, which is photographed for subsequent analysis. The signals from the photomultiplier tubes (PMT's) used to observe the light flash are also recorded photographically. When only a single PMT was used, its signal was displayed on one trace of a dual-beam oscilloscope while the detector signal was displayed on the other. When several tubes were in use simultaneously, each signal was displayed on a separate oscilloscope trace. All of the oscilloscopes were triggered from a common source (either the detector signal itself or the output signal from the velocity selector system described below) to ensure time correlation of the observed signals.

Most of the high-velocity data (i.e., above about 10 km/sec) were obtained with the aid of a recently developed velocity-selection system. The carbonyl iron particle source is characterized by a wide distribution of particle sizes (with diameters from about 0.1 to 3.0 microns). As a consequence of the charging process, the smaller and less frequently occurring particles achieve the highest velocities. Since the very high velocity particles appear so rarely, direct photography of each particle signal is not a very satisfactory way of acquiring high-velocity data. To alleviate this problem, the velocity-selection system is used to produce a trigger pulse whenever a particle within a predetermined velocity interval appears. This is accomplished by means of two particle-detection stations and a simple logic circuit. The signal from the first detector opens a narrow gate at some predetermined delay time. The signal from the second detector is fed to the gate; if the gate is open, a trigger pulse is generated but if the signal arrives at any other time no signal is generated. Both the delay time and the width of the gate pulse are adjustable. In practice, the trigger pulse is used to trigger the sweep circuits of the oscilloscopes, which display the signals from a third particle detector and the PMT's. The particle velocity and mass are determined by analysis of the signal from the third detector.

B. Impact-Flash Measurement Techniques

For the single-PMT measurements of the impact flash from glass targets, particles from the accelerator passed through a particle detector and then struck a glass target whose surface was normal to the direction of the particle beam. The target, which was in the form of a disc, also served as a vacuum window. The PMT was optically coupled to the rear of the window with Dow-Corning 200 Fluid. In some cases, the front surface of the target-window was coated with an extremely thin but opaque film of aluminum. The purpose of the film was to shield the PMT from light emitted from the vapor cloud, thus limiting these measurements to the "body flash". Under these circumstances the signal

from the PMT appears as a large amplitude spike followed by a lower-level, exponentially decreasing signal. It is presumed that the spike represents the body flash. Experiments appear to bear this out, since the amplitude of the initial spike is essentially unaltered by the presence or absence of the aluminum film.

Most of the front-surface impact-flash measurements and all of the spectral measurements were made using the target chamber shown in Fig. 1. This chamber provides viewing ports for four PMT's, which view the surface of the target at an angle of 45° to the normal. Particles from the accelerator enter the chamber through the aperture between the phototubes and impact at the center of the target, the point of impact lying at the apex of the pyramid formed by the axes of the viewing ports. The viewing ports are sealed by thin Lucite windows. The PMT's are held against the viewing ports by an aluminum structure that also has a recess for standard 2 x 2 inch optical filters. The internal surfaces of the chamber are polished to increase light-gathering efficiency, and all optical joints are made with a thin layer of silicon grease to reduce light losses at the interfaces.

RCA 6199 photomultiplier tubes with S-11 spectral response were used for all of the measurements. Standard PMT circuitry was used, with the photocathode at about 1000 volts negative and the anode grounded through the load resistor. A high-impedance voltage divider supplied the correct operating voltage to the dynodes. The last few stages were backed up by capacitors to avoid nonlinearities arising from large signal levels. The frequency response was adjusted by varying the anode capacitance to ground. The output signals were fed to wide-bandpass cathode-followers and from there directly to the oscilloscopes.

Although the PMT's were not calibrated against a standard blackbody radiation source, a certain amount of care was taken in determining the over-all response. The most critical factors affecting over-all response are the spectral response of the PMT-

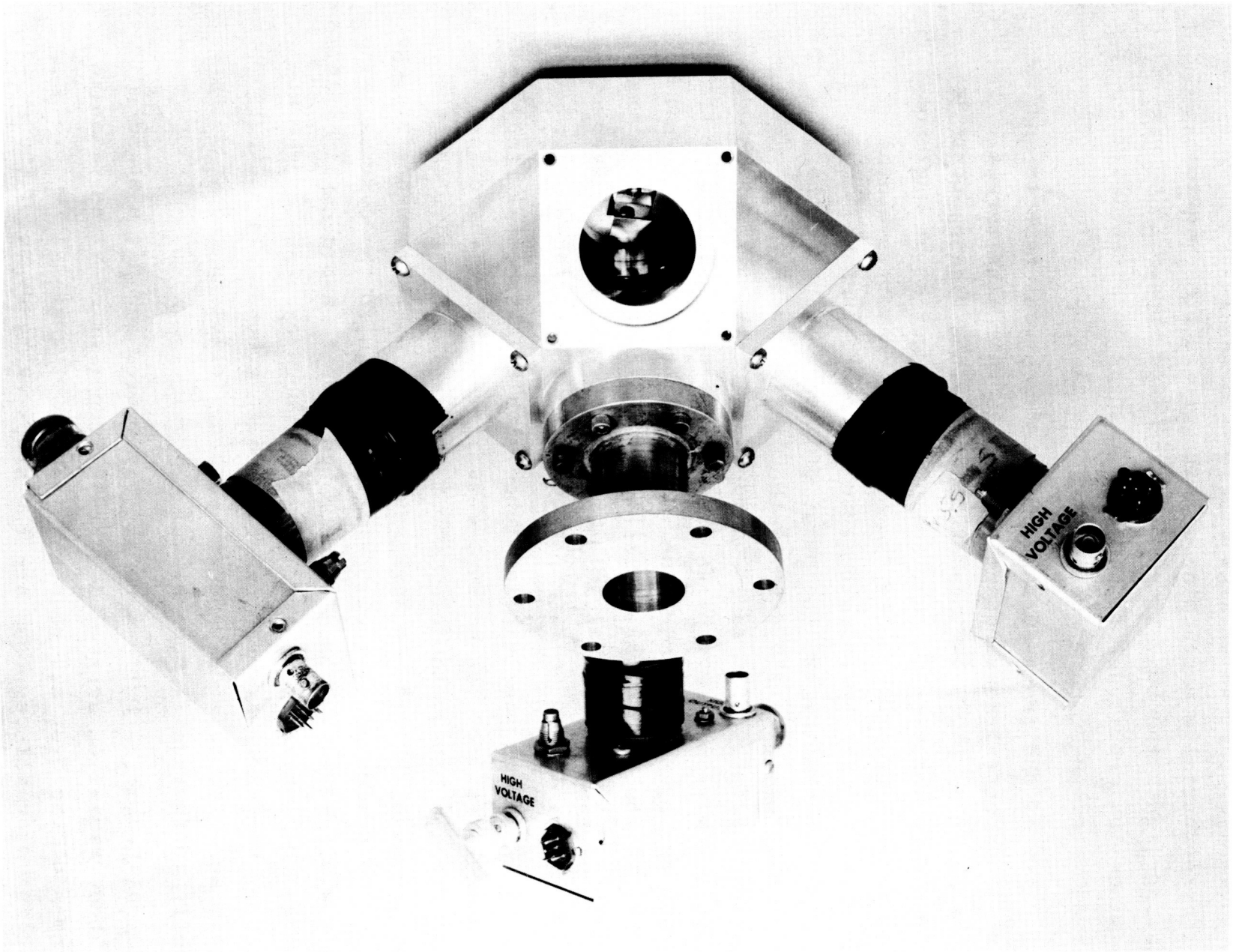

Figure 1. Impact Light Flash Target Chamber Assembly.

filter combination and the gain of the electron-multiplier assembly.

The spectral response characteristics of the PMT-filter combinations were determined from the S-11 spectral characteristics curve published by the manufacturer and from the transmission characteristics of the filters (also supplied by the manufacturer). The spectral response of two filtered PMT's that were used as a pair for the photometric measurements are shown in Fig. 2. Another pair of filtered PMT's with a similar, but slightly different spectral response was also used, but they are not illustrated. For purposes of analysis, it was assumed that the area under a particular curve represents the sensitivity to radiant energy at the peak wavelength.

To determine the gain of the electron-multiplier assemblies, the gains of the tubes that comprised a pair for the temperature measurements were adjusted to a common value. A pulsed neon light served as the calibrating source, and the gain was set by a potentiometer which adjusted the total voltage across the dynode chain. To account for possible variations in the light source intensity, each tube was checked several times. In practice, all four PMT's were fed from a single high-voltage power supply. Since electron multiplication is a strong function of voltage, the supply voltage was monitored continuously by a digital voltmeter and maintained at a value constant to about one part in a thousand. Under these conditions, the variation in electron gain was probably no greater than 1 or 2%.

C. Two-Color Temperature Measurements

In the experiments, the actual property measured is the intensity of light emission at two different wavelengths. To convert these measured values to the apparent temperature, the experimental data are used with the Planck blackbody radiation law, namely,

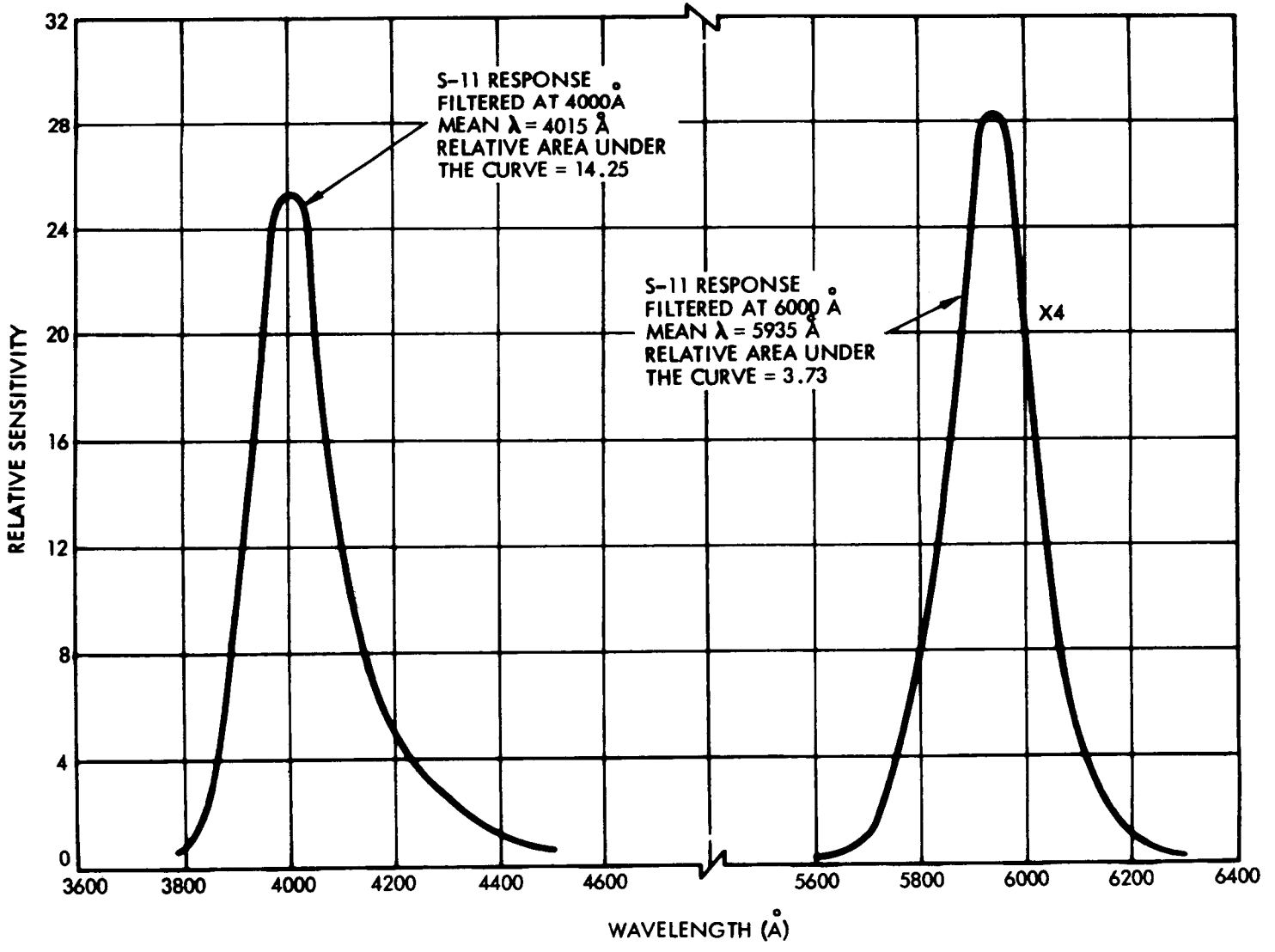

Figure 2. Spectral Response Characteristics of Two Filtered RCA 6199 Photomultiplier Tubes used as a Pair in the Two-Color Photometric Measurements.

$$\Psi_\lambda = \frac{K_1}{\lambda^5} \frac{1}{e^{(K_2/\lambda T)} - 1} \quad , \tag{1}$$

where Ψ_λ is the intensity at wavelength λ, T is the temperature of the radiator, and K_1 and K_2 are constants. The magnitude of the output signal from a PMT sensitive only at wavelength λ is given by

$$I_\lambda = S_\lambda \Psi_\lambda \quad , \tag{2}$$

where S_λ is the radiant sensitivity. The ratio of the light intensity at two different wavelengths i and j defines the temperature uniquely, as given by

$$\frac{I_i}{I_j} = \frac{S_i}{S_j} \left(\frac{j}{i}\right)^5 \frac{e^{(K_2/jT)} - 1}{e^{(K_2/iT)} - 1} \tag{3}$$

In the present case S_λ is proportional to the area under the appropriate spectral response curve. The curve for converting from measured signal level ratios to apparent blackbody temperature, as calculated from Eq. (3), is given in Fig. 3 for the spectral response characteristics indicated in Fig. 2.

III. EXPERIMENTAL RESULTS AND DISCUSSION

A. Single-Phototube Observations

As mentioned in the previous section, the body flash in glass targets is characterized by an intense, short-duration flash followed by a lower-intensity emission that decays with a relatively long time constant. The duration of the initial spike

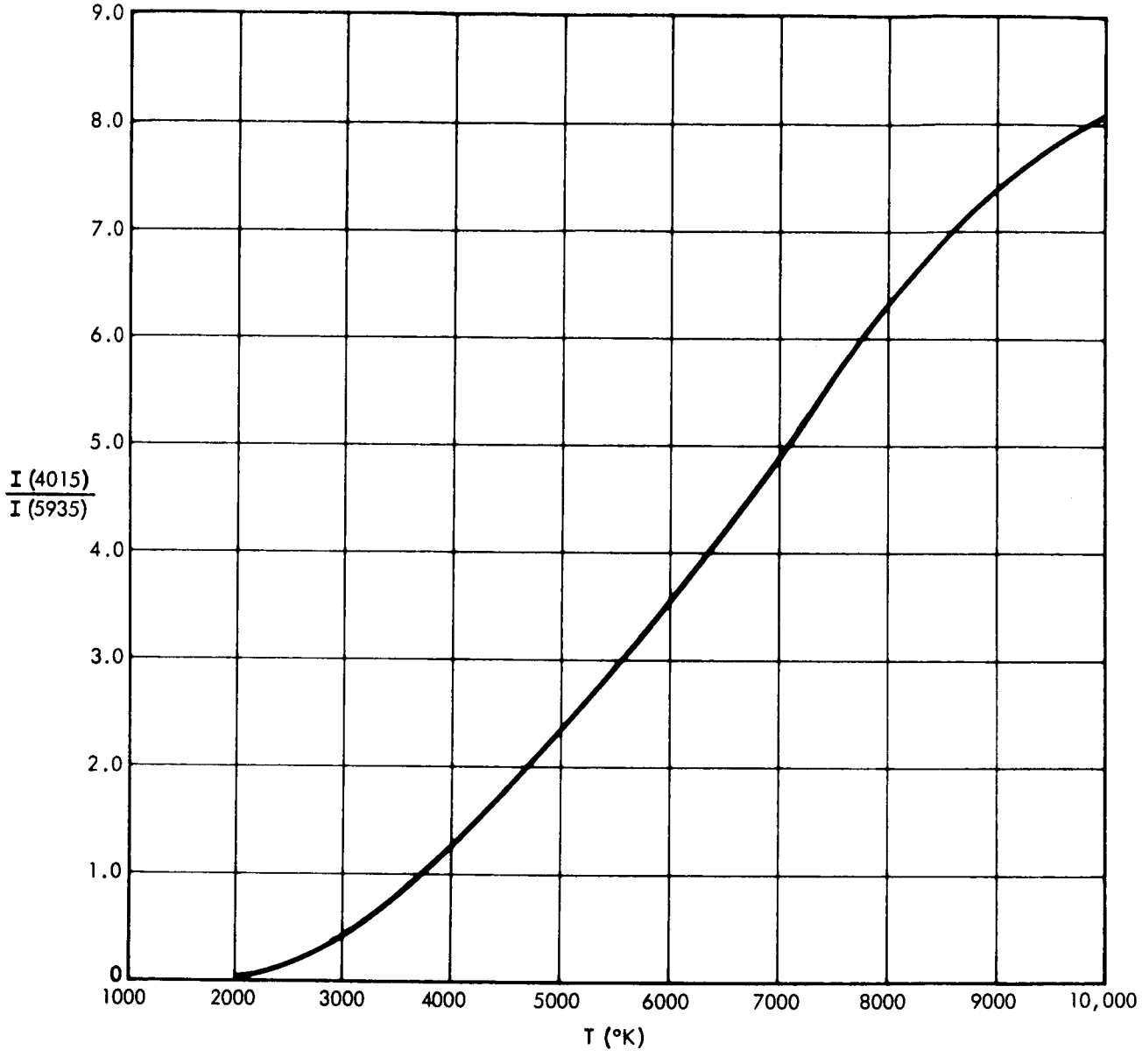

Figure 3. Calibration Curve for Conversion from Intensity Ratios to Apparent Blackbody Temperature. This curve applies to the PMT-filter combinations illustrated in Fig. 2.

is about 0.2 μsec, while the low-intensity portion of the emission persists for as long as 10 μsec. For most measurements, the PMT signal was integrated electronically to facilitate the procedures. Thus in the results obtained, the magnitude of the signal is proportional to the total radiant energy emitted but is dominated by the high-intensity portion. Typical results are illustrated in Fig. 4, where the peak light-flash amplitude divided by the mass of the particle is plotted as a function of particle velocity. Normalizing to particle mass has the effect of presenting the data as if the particles were of a uniform mass, and is based on the assumption that the magnitude of the light flash is directly proportional to particle mass.

Data for impacts on a solid tantalum target are shown in Fig. 5. In this case, of course, the impact flash was observed from the front face of the target. Again, the output signal was electronically integrated. The signal waveform observed in this manner is somewhat different in that the initial spike that is characteristic of the body flash is not nearly so prominent as that obtained with glass targets. In fact, it is questionable that it appears at all. Generally, the signal rises to peak value in about 50 nanosec and then decays exponentially with a time constant of about 5 μsec. Because of the integration, the signal amplitude is proportional to the total radiant energy within the spectral range of the PMT.

Over the limited velocity range covered by these data points, the body flash from glass targets, as represented in Fig. 4, is more strongly velocity dependent than is the flash observed from a solid metallic target. Straight-line "eye" fits to the points imply that on glass targets the body flash increases as about the seventh power of velocity, while in the other case the slope is only about three. As can be inferred from results discussed later, this difference is not attributable to the differences in target materials and hence, must be indicative of the difference between the body flash viewed from the rear of the target and

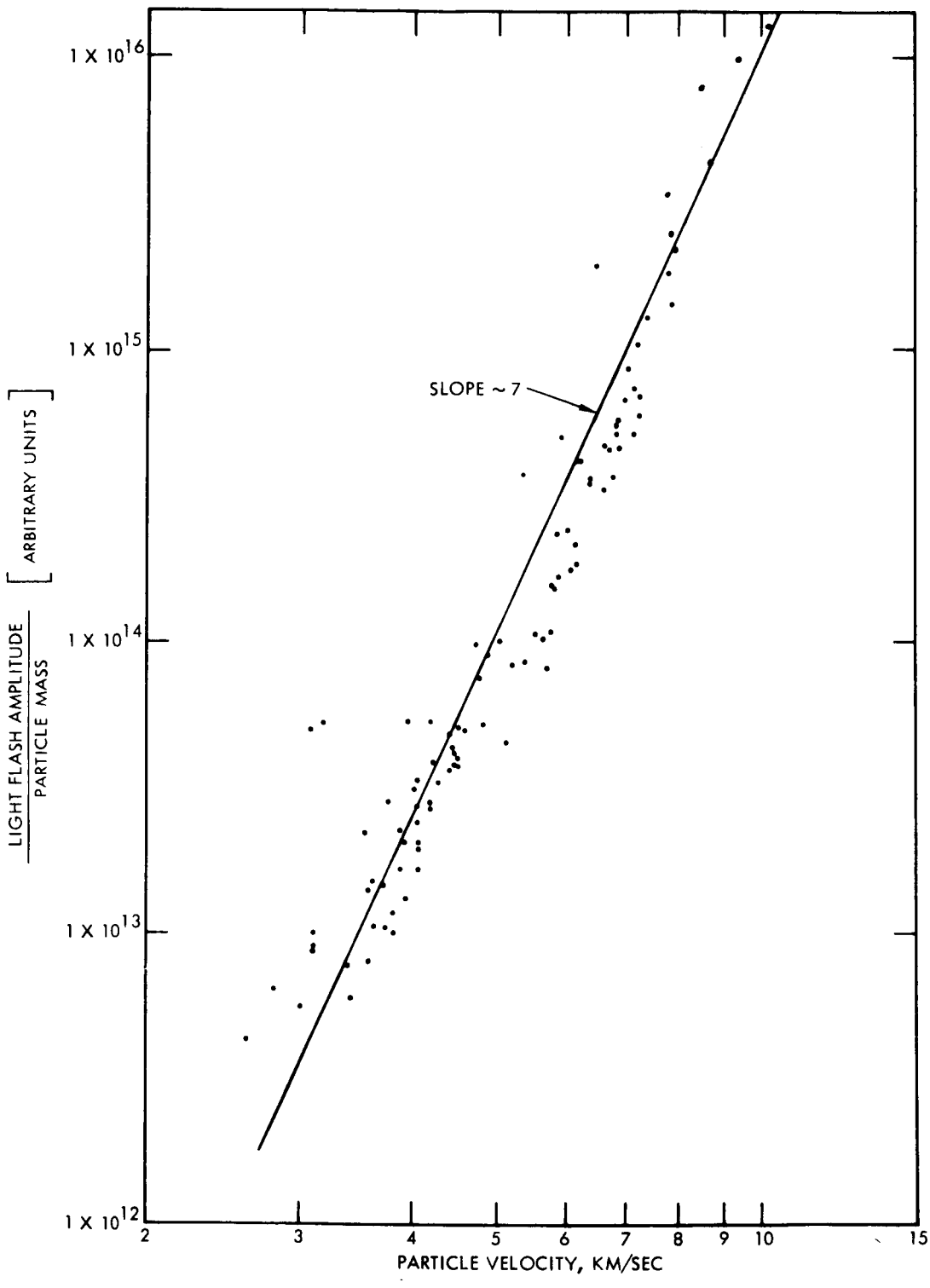

Figure 4. Light Flash Intensity over the Visible Range Normalized to Particle Mass as a Function of Impact Velocity for a Glass Target. An RCA 6199 Photomultiplier with S-11 response was used.

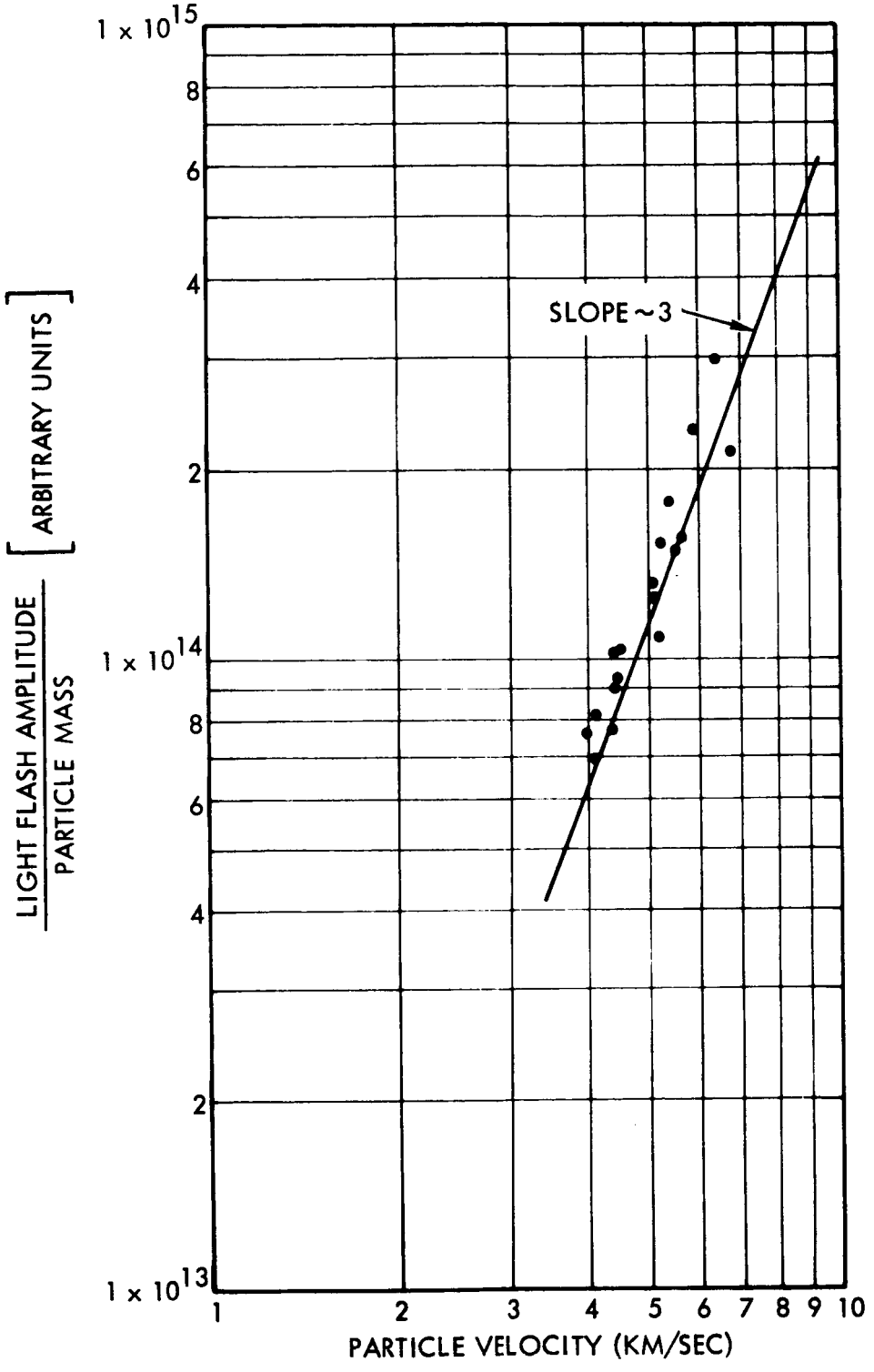

Figure 5. Normalized Light Flash Intensity as a Function of Particle Velocity obtained with a Tantalum Target and an unfiltered RCA 6199 Photomultiplier Tube.

radiation viewed from in front of the target.

B. Spectral Measurements

Two-color photometric measurements were conducted to determine apparent blackbody temperature as a function of particle impact velocity on tantalum and fused-quartz (Vycor glass) targets. The term "apparent" means that the temperature was determined on the assumption that the source of light is an ideal blackbody radiator, although there is no direct evidence to support this assumption.

Two separate temperature determinations were made for each target material. The only difference between the two test arrangements (aside from very slight differences in the spectral response of the filters used) was the output circuitry of the PMT's. For one pair of tubes the output signals were integrated by shunting the 100 KΩ anode resistors with 100 pf capacitors, giving an RC decay time of 10 μsec. In the other case, no capacitors were added and the effective RC decay times were less than 1 μsec. In the first case, the net effect of the integration is that the total radiant energy from the flash is measured at some fixed wavelength; in the second, the signal is more nearly proportional to the instantaneous radiant intensity at the wavelength specified by the spectral response characteristics of the PMT's. Since the intensity is a strong function of temperature in the range under study, the response in either case is dominated by radiation from the flash while it is at high temperature, and the peak amplitudes of the signals are representative of the maximum temperature.

In principle, the cooling of the flash could be monitored by measuring the ratio of the appropriate signals as a function of time. However, it was found that the signals decay to the noise level so rapidly that measurements of this type did not appear feasible under the present circumstances.

Generally speaking, the integrated signals provided the best-quality data, particularly at low signal levels. This

higher quality stems from the fact that the integration tends to minimize the effects of statistical fluctuations in the electron-multiplication process, which are sizable for small signals. However, measurements made with the non-integrating circuitry provide an internal check for consistency of the results.

A set of oscillographs depicting the raw data obtained for an event under somewhat favorable conditions is shown in Fig. 6. The uppermost picture shows the detector signal, while the oscillograph in the center displays the integrated output signals at 5935 Å and 4015 Å (upper and lower traces, respectively). Similar traces for the PMT's with broadband external circuitry are shown in the lower photo, where the upper trace gives the intensity at 5885 Å and the lower gives the intensity at 4050 Å.

Ideally, one needs only to measure the ratio of the amplitudes of the pair of signals to determine the apparent temperature. A case where this was done is illustrated in Fig. 7. These data were obtained from the integrated intensity measurements on a tantalum target. Clearly, the results show a steadily increasing temperature with particle velocity. One gets the impression that the ratio of intensities is increasing more slowly at the high velocities, but the scatter in the data points prevents quantitative verification of this point. The results presented in Fig. 7 are not as satisfactory as those presented later since to obtain accurate data, high-quality signals must be obtained simultaneously from both PMT's, and this was not always the case. Often the signal from one of the two PMT's was either too large or too small to be measured accurately, and at the higher temperatures the blue-sensitive PMT produced larger and more easily measured signals, which apparently led to a high-temperature bias.

To alleviate this problem and to minimize the scatter exhibited by the points in Fig. 7, an averaging technique was employed. In this method the peak light-flash amplitude, normalized to particle mass, was plotted as a function of particle

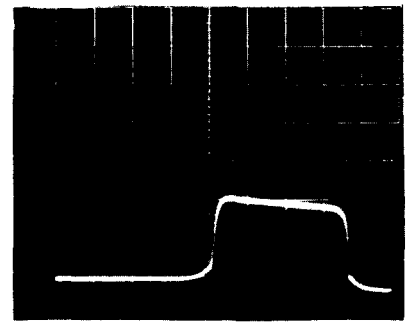

6a

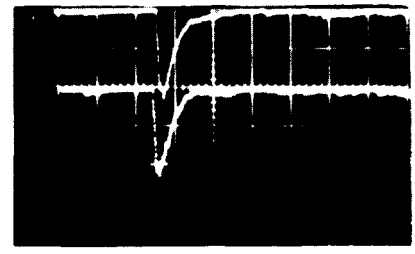

6b

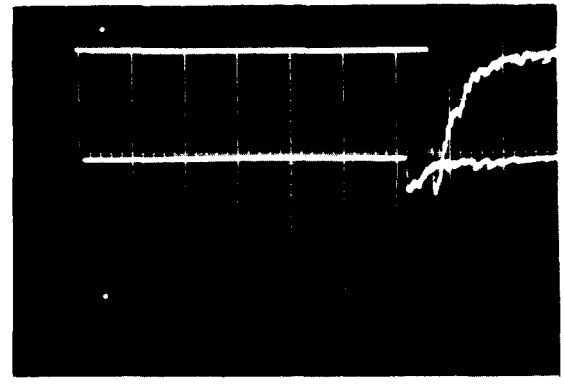

6c

Figure 6. Oscillographs Illustrating the Response of the Various Sensors. The uppermost picture shows the signal from the particle velocity-charge detector. The photograph in the center shows the signals from the PMT's with integrating output characteristics. The upper trace in this picture was derived from a PMT sensitive at 5935 Å while the lower trace corresponds to the intensity at 4015 Å. Similar signals from the PMT's with broadband external circuitry are shown in the lower picture with the upper and lower traces giving the intensity at 5885 Å and 4050 Å respectively.

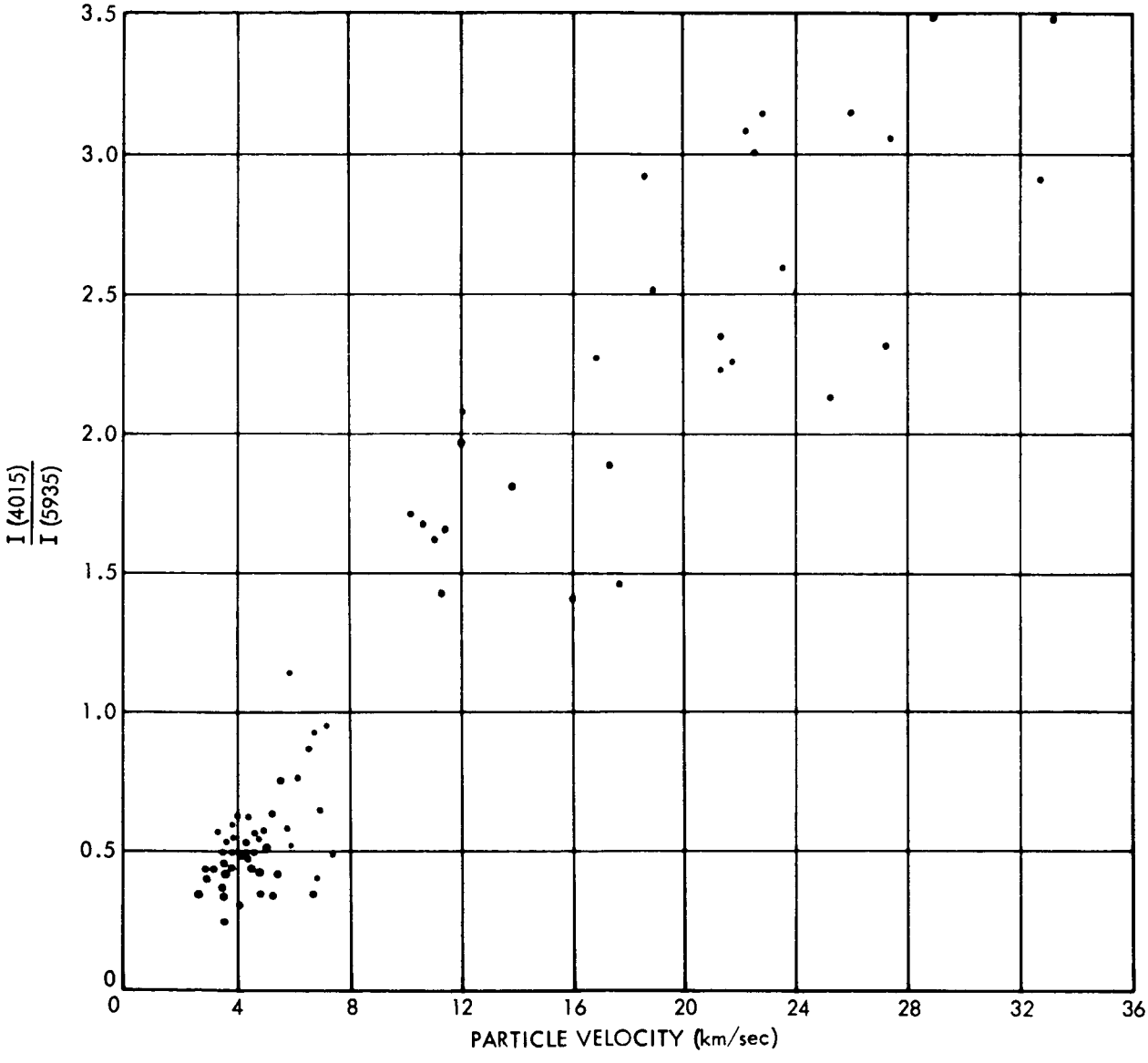

Figure 7. Direct Ratios of Impact Flash Intensity at 4015 Å and 5935 Å as a Function of Velocity for a Tantalum Target. In this case, the output signals from the PMT's were integrated.

velocity for each of the PMT's. A smooth curve was fitted to each set of data. The ratio of the values of the appropriate two curves at a selected velocity then yielded an average maximum blackbody temperature at that velocity.

The data are presented in Figs. 8 through 11. The points represent the logarithms of the measured values of the peak signal amplitude in arbitrary units normalized to the measured particle mass at the velocity indicated. The strong velocity dependence of the light flash as measured at a fixed wavelength is evident from these figures, since the light-flash amplitude increases by about 5 or 6 orders of magnitude over the velocity range covered. The curves were fitted to the data points by an iterative process. First the unweighted data were fitted to polynomials of second and third degree by standard computer methods. Gaps in the distribution of data points prevented an entirely satisfactory curve fit by this technique. Next, average values of the normalized light-flash amplitudes were determined over narrow velocity intervals, and these values were fitted by inspection. The curves defined in this manner and the computer-generated curves were compared for consistency. Obvious differences were rationalized by inspection, and the final curves as indicated in the figures were defined. Obviously, personal judgment plays a major role in defining the curves this way. Although the element of judgment precludes a quantitative estimate of the fitting errors, it is felt that the final results are quite representative of the actual temperatures involved. The final results relating apparent blackbody temperatures to impact velocity are given in Figs. 12 through 15.

As was mentioned above, the highest quality data were obtained when the output signals from the PMT's were integrated. Results obtained under these conditions are shown in Fig. 12 for a tantalum target and in Fig. 13 for the fused-quartz target. In both cases the apparent temperature increases with velocity, as might be expected, but appears to be asymptotically approaching a limiting temperature of about 5000°K. Although the problem has not

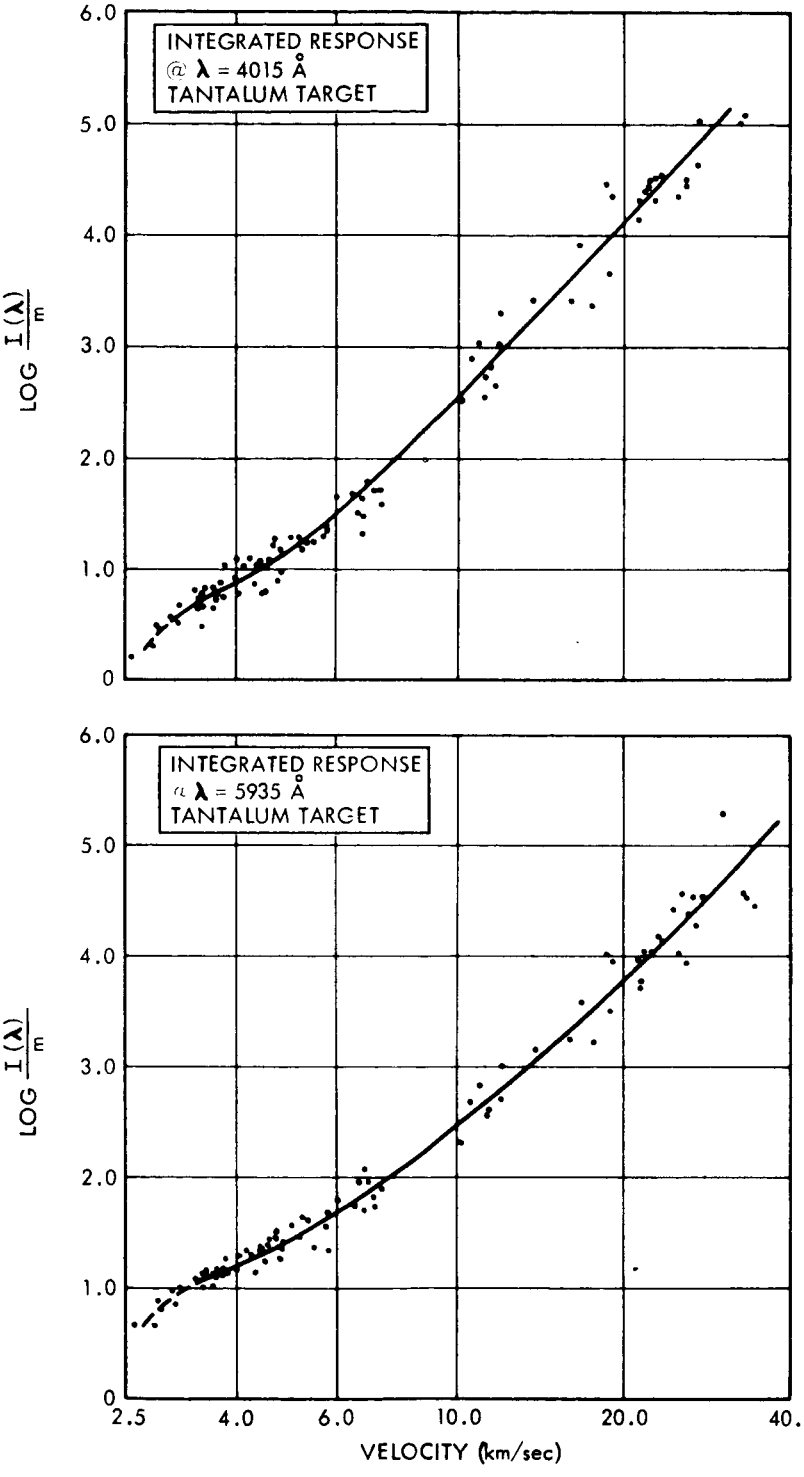

Figure 8. Logarithm of the Integrated Light Flash Intensity Normalized to Particle Mass as a Function of Velocity for PMT's Sensitive at 5935 Å and 4015 Å and a Tantalum Target.

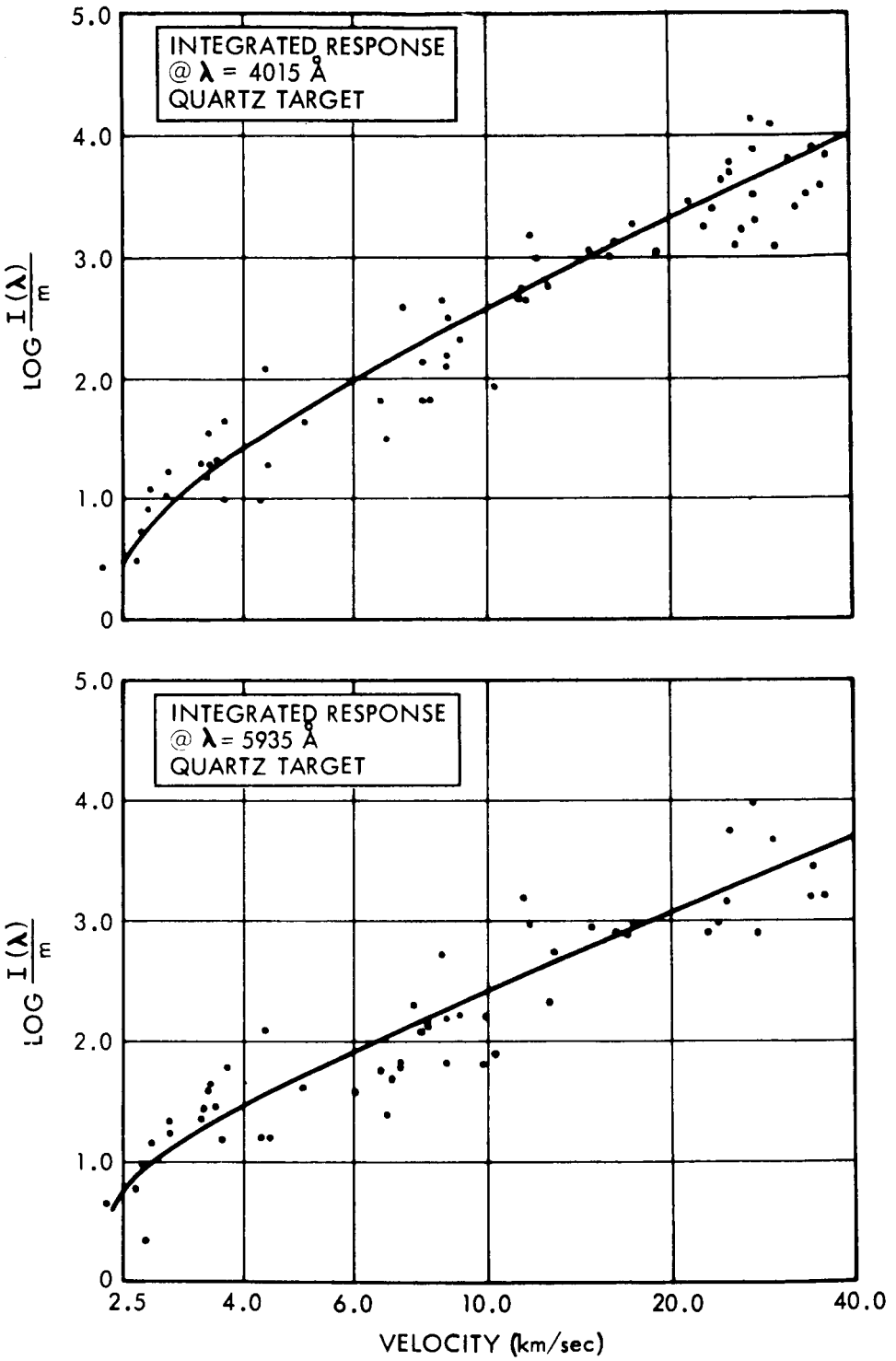

Figure 9. Logarithm of the Integrated Light Flash Intensity Normalized to Particle Mass as a Function of Velocity for PMT's Sensitive at 5935 Å and 4015 Å and a Fused-Quartz Target.

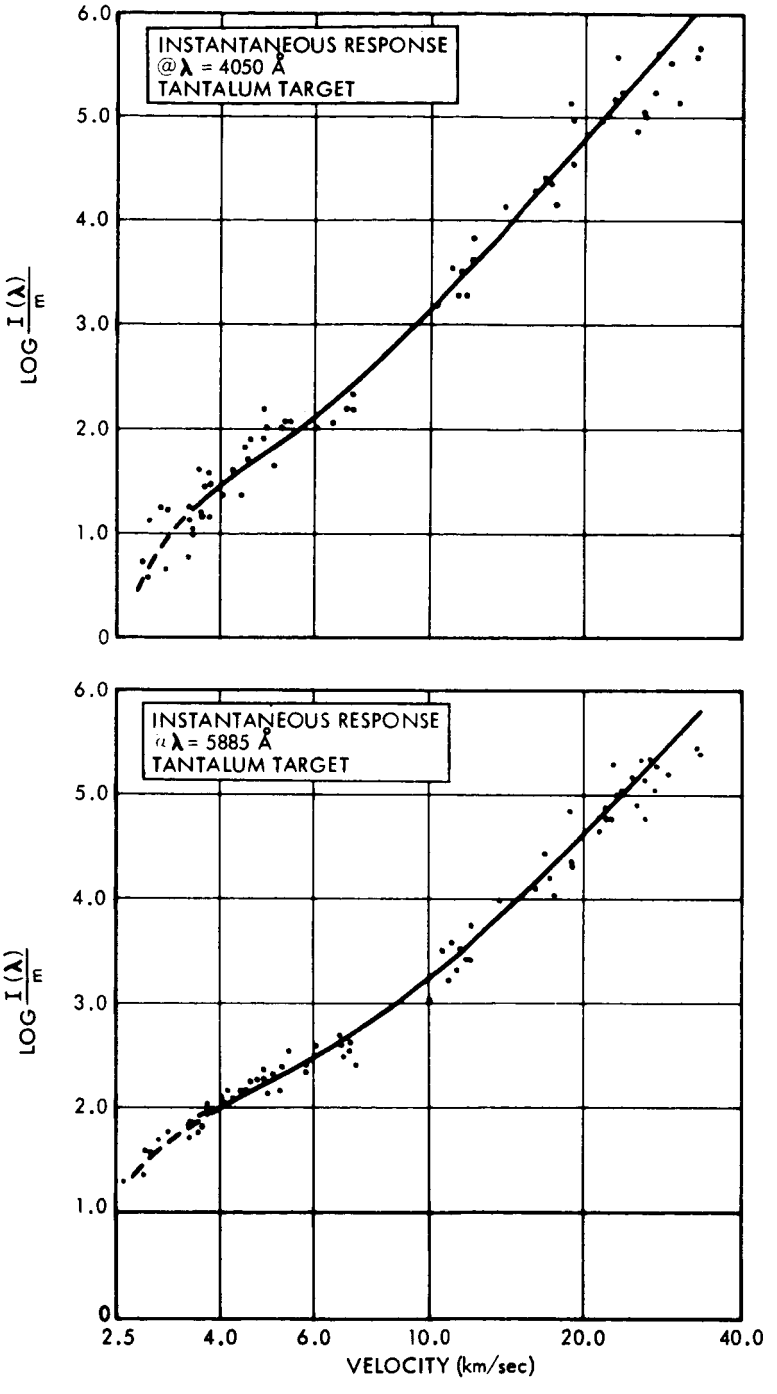

Figure 10. Logarithm of the Maximum Instantaneous Flash Intensity Normalized to Particle Mass as a Function of Velocity for PMT's Sensitive at 5885 Å and 4050 Å and a Tantalum Target.

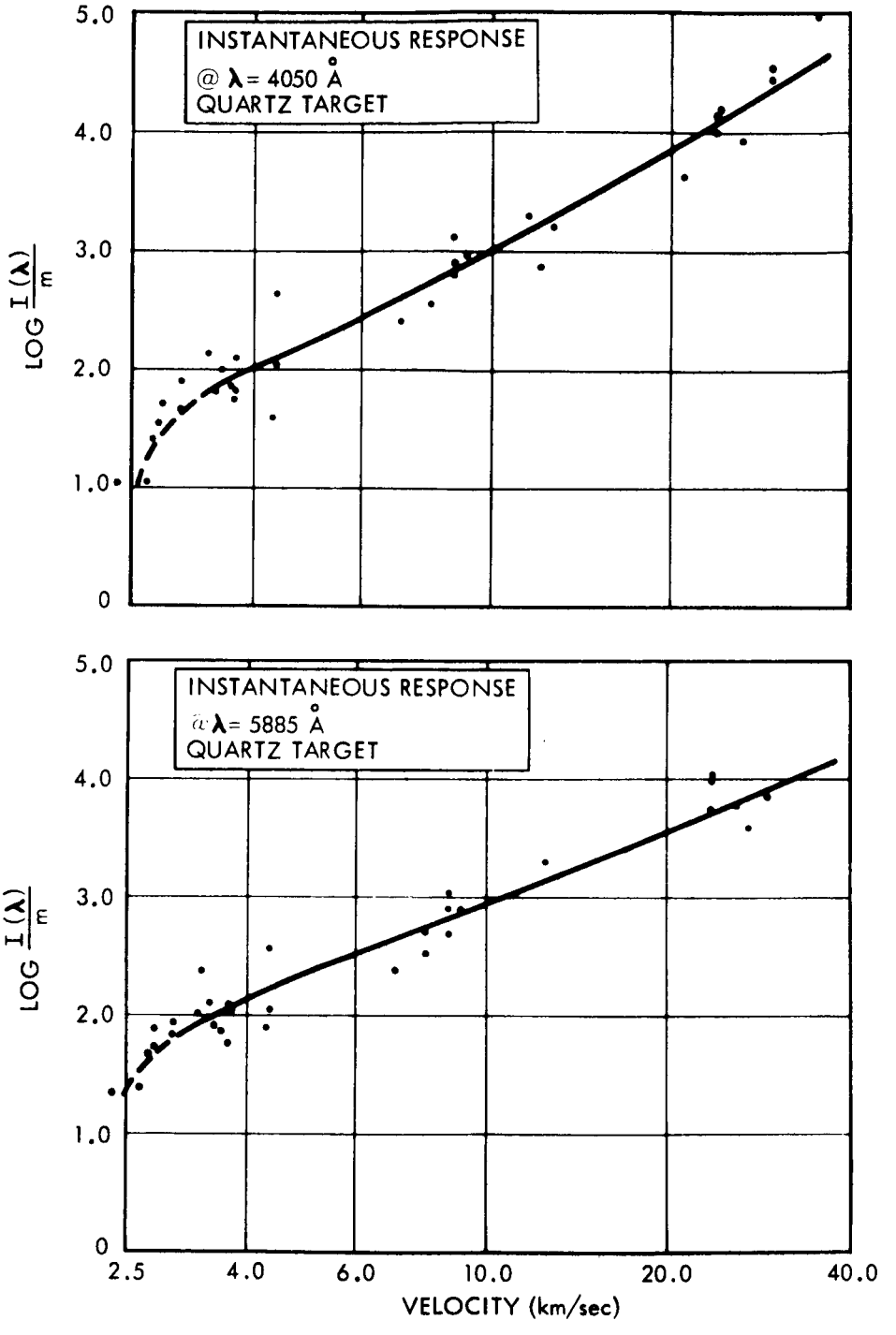

Figure 11. Logarithm of the Maximum Instantaneous Flash Intensity Normalized to Particle Mass as a Function of Velocity for PMT's Sensitive at 5885 Å and 4050 Å and a Fused-Quartz Target.

been treated analytically, it is probably safe to assume that the temperature limit is imposed by more efficient radiation cooling at higher temperatures and by the absorption of energy by competing mechanisms, such as ionization of the vapor atoms.

Although the same limiting temperature is approached for both types of targets, markedly higher temperatures are measured at low velocities with the quartz target. The lower heat conductivity of quartz may account for this effect, since the energy release is confined to a smaller volume of material at a correspondingly higher temperature. The apparent difference in measured temperatures at about 3 km/sec and below is probably the result of uncertainties in the curve fitting procedure rather than any actual difference. Also, the radiation levels in this region barely exceed the threshold for detection.

The temperature measurements made with the wideband-response PMT's are shown in Figs. 14 and 15 for the tantalum and quartz targets, respectively. Generally, the results obtained are similar to those discussed above; however, the curves are more complicated in form. It is felt that this difference arises from uncertainties in fitting the individual curves to the data points. For example, the increase in temperature indicated at about 25 km/sec in Fig. 14 arises from a small number of data points and may represent only a statistical fluctuation.

It is interesting to compare the results here with the results of similar experiments conducted by Rosen and Scully (Ref. 2). In their experiments the apparent blackbody temperature was measured for glass particles impacting on a lead target over the velocity range of about 4 to 15 km/sec. They found that the data, when plotted in the same form as shown in Fig. 12, could be fitted by a straight line, which implies that the ratio of intensities is proportional to the impact velocity raised to some power. Over the same velocity range, a straight line would provide a reasonably close approximation to the segment of the curve shown in Fig. 12. Furthermore, the maximum temperature they measured

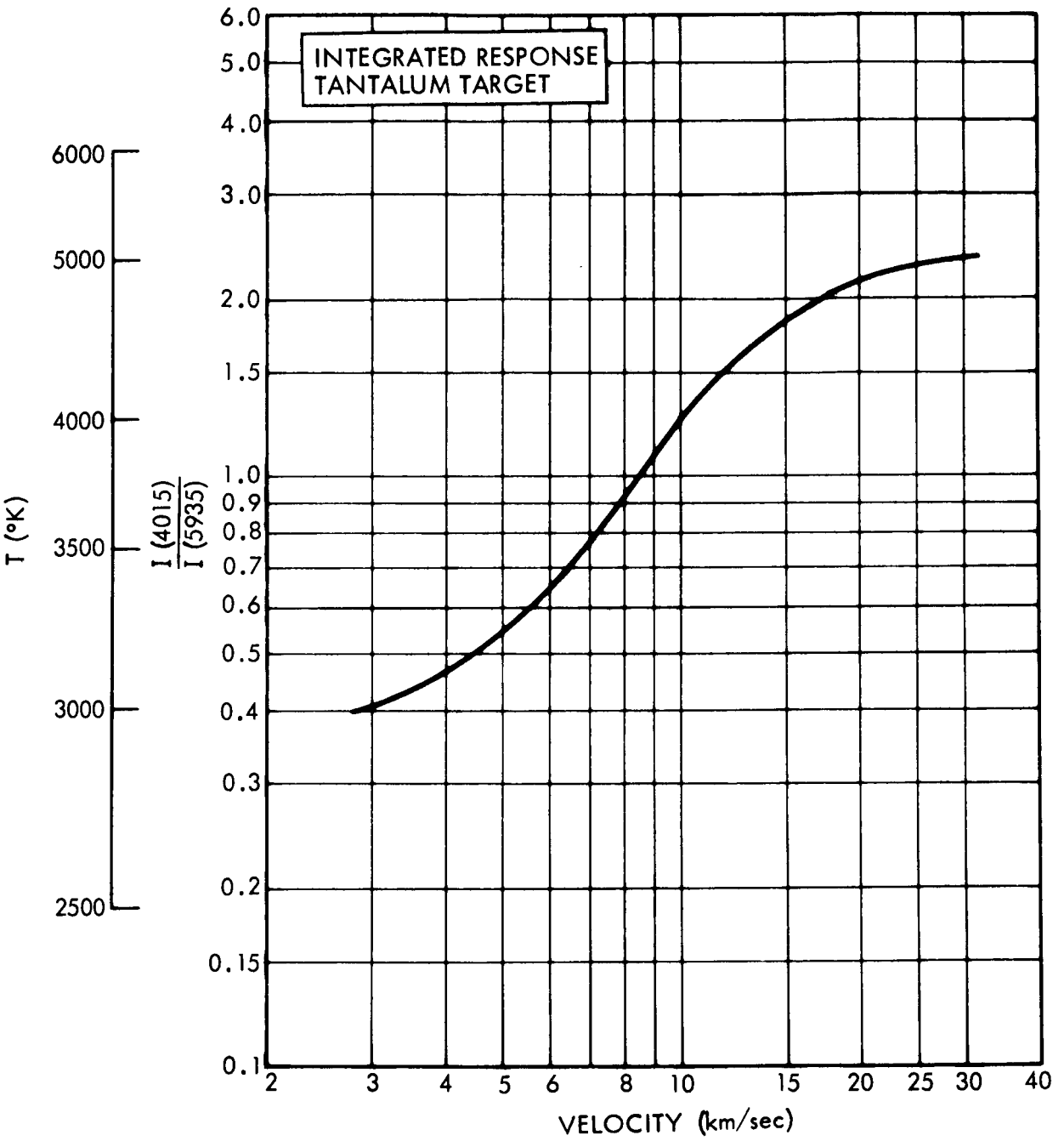

Figure 12. Apparent Blackbody Temperature of the Impact Light Flash as a Function of Particle Velocity obtained from Integrated Light Intensity Measurements on a Tantalum Target.

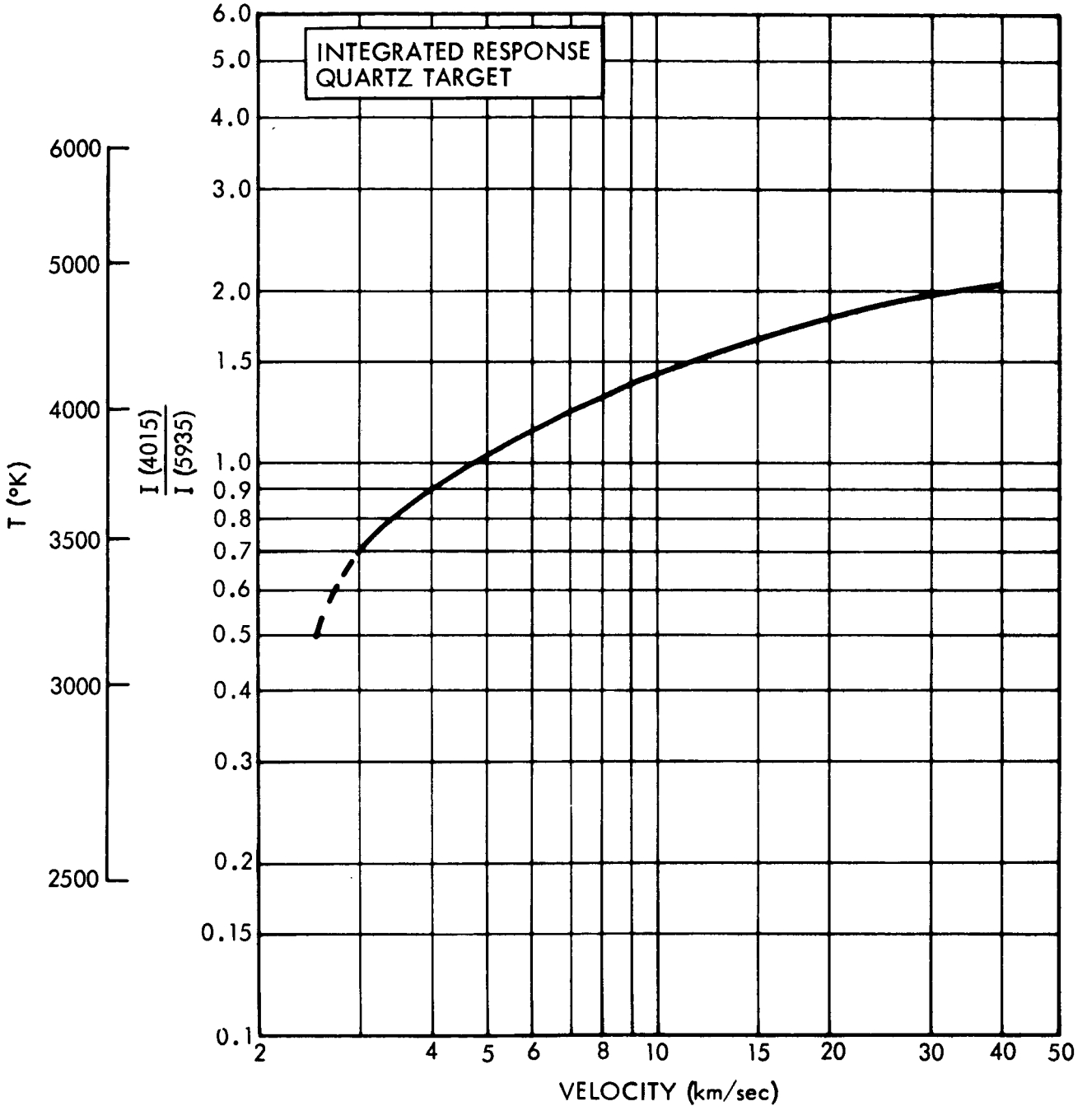

Figure 13. Apparent Blackbody Temperature of the Impact Light Flash as a Function of Particle Velocity obtained from Integrated Light Intensity Measurements on a Fused-Quartz Target.

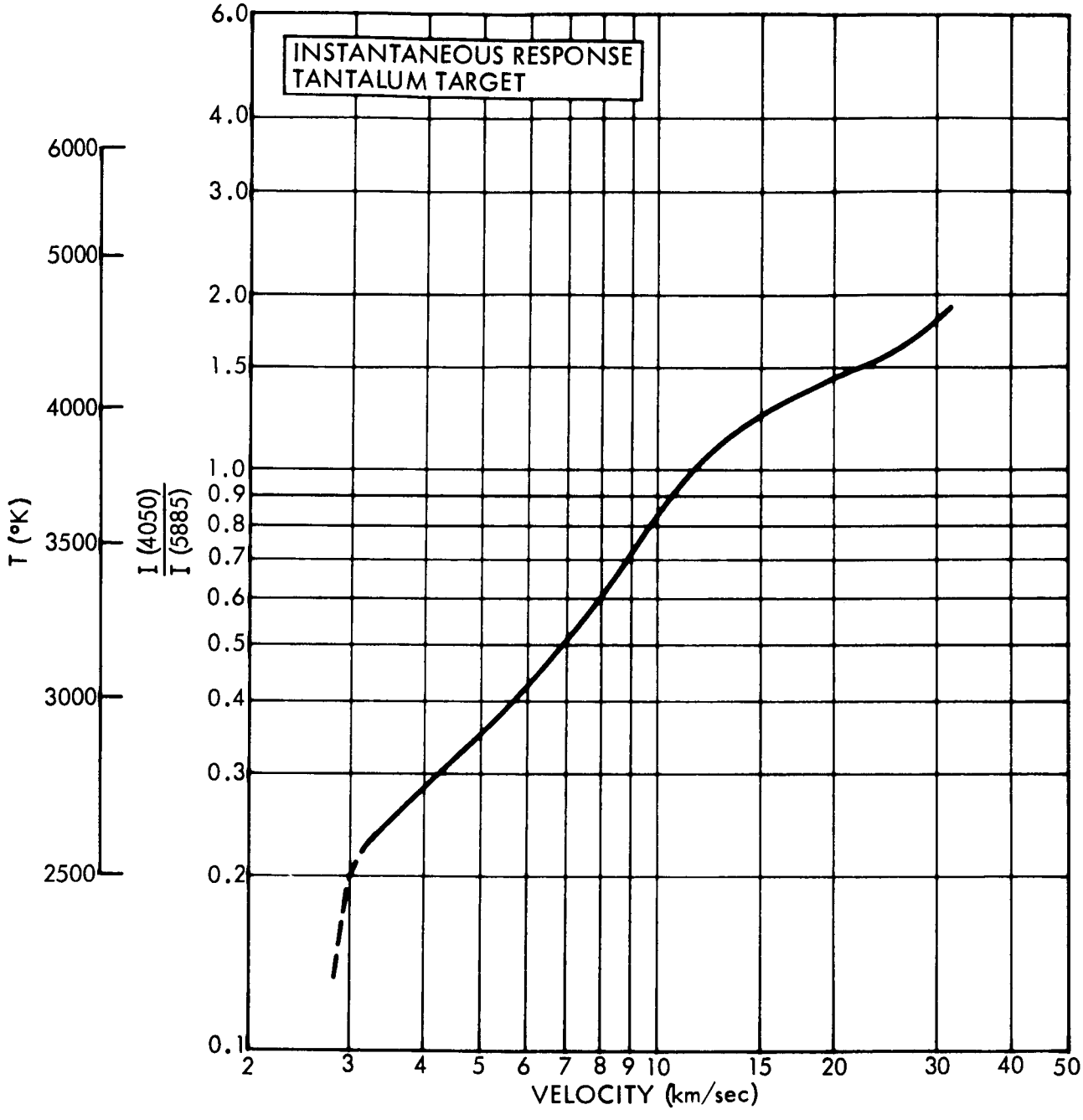

Figure 14. Apparent Blackbody Temperature of the Impact Light Flash as a Function of Particle Velocity obtained from Maximum Instantaneous Flash Intensity Measurements on a Tantalum Target.

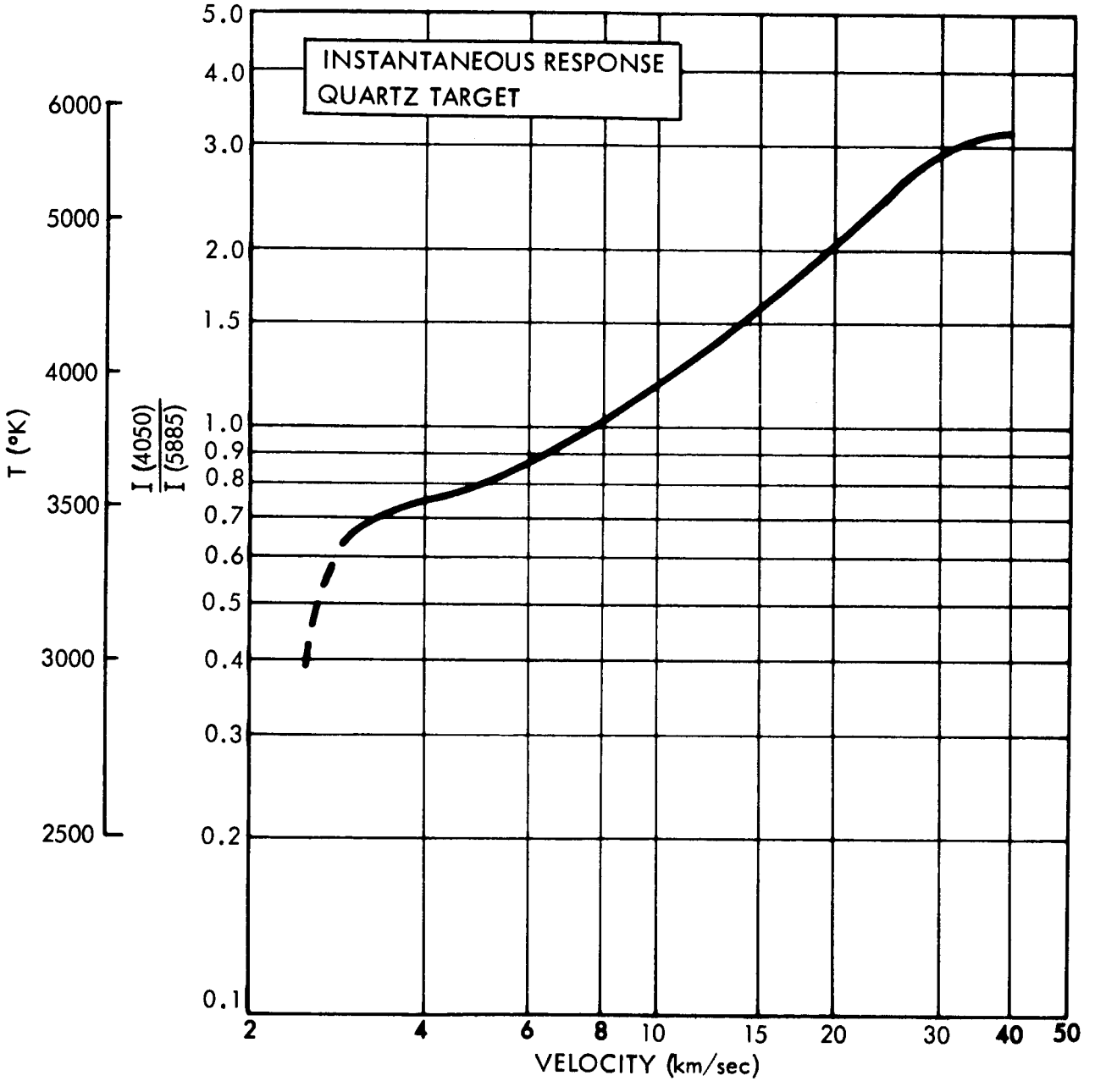

Figure 15. Apparent Blackbody Temperature of the Impact Light Flash as a Function of Particle Velocity obtained from Maximum Instantaneous Flash Intensity Measurements on a Fused-Quartz Target.

was about 5000°K, which is nearly identical to the maximum temperature measured here. Thus the results from the two experiments are compatible over the velocity range where direct comparison is valid. However, results obtained with higher-velocity particles show conclusively that the extrapolation to meteoric velocities suggested by Rosen and Scully is not valid.

IV. SUMMARY

The experiments described above have extended measurements on the impact light flash to particle velocities of nearly 40 km/sec. The very strong velocity dependence exhibited by the impact flash suggested that the source of light was similar to a blackbody radiator. On this assumption, two-color photometric measurements designed to determine an "apparent" blackbody temperature were conducted. The results indicate that the apparent temperature increases rapidly up to about 15 km/sec. At higher velocities the rate of temperature increase is smaller and asymptotically approaches a value of about 5000°K. The results obtained here are in good agreement with the results of Rosen and Scully over the velocity range common to both experiments.

As suggested earlier, the results here are related to meteorite detection systems and to basic studies of hypervelocity impact phenomena. Clearly, additional work, both theoretical and experimental, is required to correlate the results obtained here with other properties of high-speed impact.

REFERENCES

1. O. E. Berg and L. H. Meridith, Journal of Geophysical Research, Vol. 61, 751 (1956).

2. F. D. Rosen and C. N. Scully, Proceedings of the Seventh Hypervelocity Impact Symposium, Vol. VI, Published by the Martin Company, Orlando, Florida, February, 1965.

3. R. L. Bjork, Proceedings of the Sixth Hypervelocity Impact Symposium, Vol. II, Published by the Firestone Tire and Rubber Co., Cleveland, Ohio, August, 1963.

4. C. J. Maiden, J. W. Gehring, and A. R. McMillan, "Investigation of Fundamental Mechanisms of Damage to Thin Targets by Hypervelocity Projectiles," Final Report TR 63-225, September, 1963.

5. J. F. Friichtenicht and J. C. Slattery, "Ionization Associated with Hypervelocity Impact," NASA Technical Note TN D-2091, August, 1963.

6. R. W. Grow, R. R. Kadesch, E. P. Palmer, W. H. Clark, J. S. Clark, and R. E. Blake, Proceedings of the Fourth Hypervelocity Impact Symposium, Published by Air Proving Ground Center, Eglin Air Force Base, Florida, September, 1960.

7. J. F. Friichtenicht, Rev. of Sci. Instr., Vol. 33, 209 (1962).

8. H. Shelton, C. D. Hendricks, Jr., R. F. Wuerker, Journal of Appl. Phys., Vol. 31, 1243 (1960).